TORSION OF RECTANGULAR CONNECTION ELEMENTS

BO DOWSWELL

ABSTRACT

Traditionally, the torsional design of rectangular members has been based on elastic calculations. For member design, this approach is justified because beams subjected to torsion are usually controlled by torsional rotation serviceability limits. However, designs that are based on a first yield criterion underestimate the strength of connection elements. To evaluate the true torsional behavior of connection elements, various factors affecting the torsional strength of short rectangular members are investigated, showing that the torsional strength of connection elements can be predicted with rational analysis models using an ultimate strength approach.

The torsional strength of connection elements can be attributed to the resistance due to uniform torsion, warping torsion, and the Wagner effect. A method is proposed for calculating the strength of rectangular connection elements subjected to any possible combination of loads, including torsion. The design method results in a significant increase in torsional strength compared to traditional analysis methods. The method can be used to analyze extended single-plate connections subjected loads in any direction, including axial forces and combined vertical and horizontal shear forces. Three design examples show the proper application of the design method.

Keywords: torsion, torsional strength, torsional rotation, warping, rectangular connection elements, ultimate strength.

INTRODUCTION

Traditionally, the torsional design of rectangular members has been based on elastic calculations. For member design, this approach is justified because beams subjected to torsion are usually controlled by torsional rotation serviceability limits. However, designs that are based on a first-yield criterion underestimate the strength of connection elements.

For extended single-plate connections, the elastic uniform (Saint Venant) torsion strength was used by Sherman and Gorbanpoor (2002) to develop a proposed design equation for the limit state of torsion. More recently, Thornton and Fortney (2011) derived an equation to calculate the torsional strength of extended single-plate connections using the plastic uniform torsion strength. Dowswell (2015) proposed an interaction equation for the plastic strength of rectangular connection elements subjected to various loads, including torsion.

Although the theoretical plastic uniform torsion strength is 50% greater than the elastic strength (Dowswell, 2015), an evaluation of the existing research on extended single-plate shear connections revealed strengths much higher than the plastic uniform torsion strength. Additionally, experiments on single-plate connections subjected only to torsion (no shear or moment), showed that the connection torsional strength greatly exceeds the uniform torsion strength (Bennets et al., 1981).

To evaluate the true torsional behavior of connection elements, various factors affecting the torsional strength of short rectangular members are investigated in this paper. The purpose of this paper is to show that the torsional strength of connection elements can be predicted with rational analysis models using an ultimate strength approach. A design method based on these models, including the interaction of torsion with other loads, is proposed. The results from practical connections are evaluated and compared to existing analysis methods, and three design examples show the practical implementation of the proposed design method.

UNIFORM TORSION

For uniform torsion, also known as Saint Venant torsion, the applied torque is resisted by shear stresses distributed over the cross section. The uniform torsional moment is

$$T_u = GJ\theta' \tag{1}$$

For uniform members with constant torque along the length, $\theta' = \theta/L$. The torsional constant for a rectangular member is

$$J = k_u d t^3 \tag{2}$$

where $k_u = ⅓ - 0.2t/d$ for $d/t < 10$ and $k_u = ⅓$ for $d/t \geq 10$ (Seaburg and Carter, 1997). The first-yield torsional moment is

$$T_{uy} = \frac{\tau_y J}{t} \tag{3}$$

Bo Dowswell, P.E., Ph.D., Principal, ARC International, LLC, Birmingham, AL. Email: bo@arcstructural.com

Paper No. 2017–06R

For $d/t \geq 10$, which satisfies the geometry for most connection elements,

$$T_{uy} = \frac{\tau_y d t^2}{3} \quad (4)$$

For uniform members with constant torque along the length, the elastic rotation is

$$\theta_u = \frac{T_u L}{GJ} \quad (5)$$

The yield rotation is

$$\theta_{uy} = \frac{\tau_y L}{Gt} \quad (6)$$

The plastic uniform torsion strength is

$$T_{up} = \frac{\tau_y d t^2}{2} \quad (7)$$

where

F_y = specified minimum yield strength, ksi
G = shear modulus of elasticity = 11,200 ksi
J = torsional constant, in.^{4}
L = member length, in.
T_u = uniform torsional moment, kip-in.
d = member depth, in.
t = member thickness, in.
z = distance along the member length, in.
τ_y = shear yield stress = $0.6F_y$, ksi
θ = angle of rotation, rad
θ' = angle of rotation per unit length, first derivative of θ with respect to z, rad

By comparing Equation 4 to Equation 7, it can be seen that $T_{up} = 1.5T_{uy}$. The torsional stiffness is linear up to the yield moment, T_y, and then the curve becomes nonlinear up to a maximum value of $T = T_{up} = 1.5T_{uy}$, as shown in Figure 1 (Dowswell, 2015).

WARPING

Except for circular cross sections, warping is present in all members subjected to torsion. Warping is classified as either primary or secondary. For primary warping, torsion is resisted by stresses across the element depth, and secondary warping is where torsion is resisted by stresses across the element thickness. For most members, any resistance developed through secondary warping is insignificant compared to uniform torsion and primary warping resistances.

For typical rectangular members, warping is negligible compared to uniform torsion. Therefore, the common practice of neglecting any warping contribution for rectangular members is justified. However, warping can provide significant torsional resistance to connection elements where the length is relatively short compared to the cross-sectional dimensions. This behavior was shown by Reissner and Stein (1951), who solved the differential equation of a rectangular cantilever plate subjected to a concentrated torsional moment at the free end, and by Baba and Kajita (1982), who developed inelastic finite element models of rectangular cantilever members subjected to a free-end concentrated torsion.

Elastic Strength

The elastic warping behavior can be analyzed using AISC Design Guide 9, *Torsional Analysis of Structural Steel Members* (Seaburg and Carter, 1997). The warping torsional moment is

$$T_w = -EC_w\theta''' \quad (8)$$

The warping constant for a rectangular member is

$$C_w = k_w d^3 t^3 \quad (9)$$

For narrow rectangles with $d/t \geq 10$ (Gjelsvik, 1981)

$$k_w = \frac{1}{144} \quad (10)$$

For rectangular members with $d/t < 10$ (Balaz and Kolekova, 2002)

$$k_w = \frac{1}{144}\left[1 - 4.88\left(\frac{t}{d}\right)^2 + 4.97\left(\frac{t}{d}\right)^3 - 1.07\left(\frac{t}{d}\right)^5\right] \quad (11)$$

Figure 2 shows warping stress distributions for elastic warping, inelastic warping and plastic warping. The maximum value for the elastic warping normal stress distribution

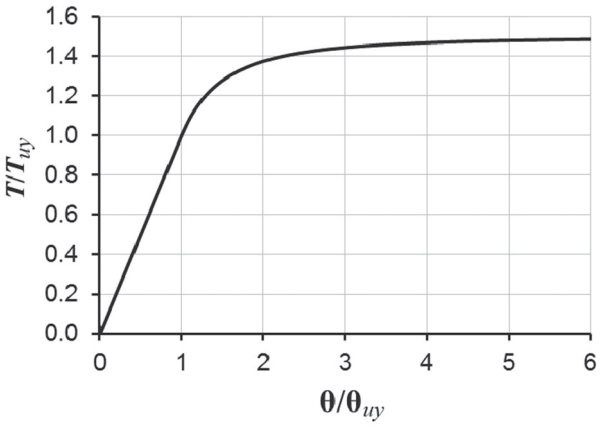

Fig. 1. Normalized torsion versus normalized angle of twist (Dowswell, 2015).

as shown in Figure 2(a), which occurs at the corners, is

$$\sigma_{wc} = EW_{nc}\theta'' \tag{12}$$

The normalized warping function at the corner of the cross section is

$$W_{nc} = \frac{dt}{4} \tag{13}$$

where

C_w = warping constant, in.^{6}
E = modulus of elasticity, ksi
W_{nc} = normalized warping function at the corner of the cross section, in.^{2}
θ'' = second derivative of θ with respect to z, rad
θ''' = third derivative of θ with respect to z, rad

Figure 3 shows the deformed shape of a single-plate connection subjected to twisting (Sherman and Ghorbanpoor, 2002; Moore and Owens, 1992; Abou-Zidan, 2014; Suleiman, 2013). The double-curvature along the length indicates that warping is fixed at both ends of the plate.

Case 2 in AISC Design Guide 9, Appendix B, provides charts for determining θ, θ', θ'' and θ''' for members subjected to concentrated end torques with warping fixed at each end. The values can also be calculated with the equations in Moore and Mueller (2002). The maximum warping stresses are at the member ends ($z = 0$ and $z = L$), where the equation for θ'' reduces to

$$\theta'' = \frac{T}{GJa}\tanh\left(\frac{L}{2a}\right) \tag{14}$$

where

$$a = \sqrt{\frac{EC_w}{GJ}} \tag{15}$$

T = torsional moment, kip-in.

Isolated Flange Method

Gjelsvik (1981) showed that the elastic torsional moment is statically equivalent to a couple formed of two equal and opposite out-of-plane forces, F, acting on each half of the cross section at $h = 2d/3$, as shown in Figure 4(a). Gjelsvik's equivalent couple can be expanded to simplify warping calculations for connection elements, where only the shaded portion of the cross section on each half of the member depth is effective in resisting force, F. The equivalent cross-section $t \times \alpha d$ is modeled as a flexural member of length L with the fixed-slider boundary conditions shown in Figure 4(b). The required moment at each end of the member is

$$M_{re} = \frac{FL}{2} \tag{16}$$

This isolated-flange analysis method is common in the torsional analysis of I-shaped members, where the flanges are isolated and treated as flexural members to calculate the warping strength.

For elastic stresses, $\alpha = 1/4$ and the out-of-plane force, F, is

$$F = \frac{3T_w}{2d} \tag{17}$$

The weak-axis yield moment of the equivalent beam, M_{ye}, is

$$M_{ye} = \frac{F_y \alpha d t^2}{6} \tag{18}$$

Setting Equation 16 equal to Equation 18 and solving for F results in the out-of-plane force required to initiate first yield, F_{wy}.

$$F_{wy} = \frac{F_y \alpha d t^2}{3L} = \frac{F_y d t^2}{12L} \tag{19}$$

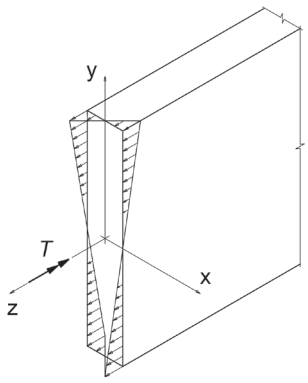

(a) elastic

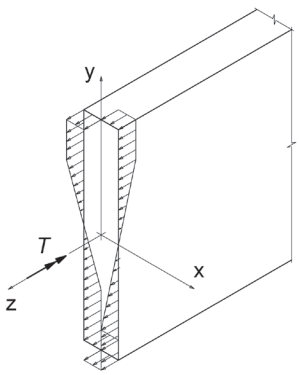

(b) inelastic

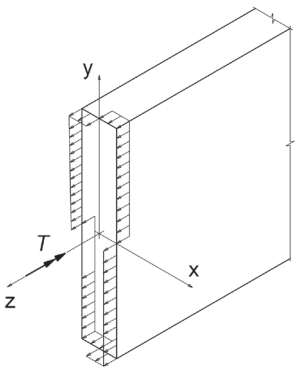

(c) plastic

Fig. 2. Warping stresses.

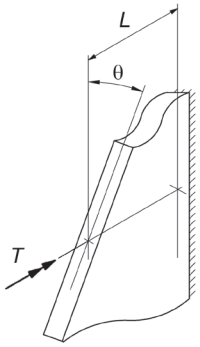

Fig. 3. Torsional deformation of a connection element.

Setting Equation 17 equal to Equation 19 and solving for T_w results in the warping torsion required to initiate first yield.

$$T_{wy} = \frac{F_y d^2 t^2}{18L} \tag{20}$$

The rotation can be estimated from the free-end deflection of the equivalent beam, δ, shown in Figure 4(b). The end deflection is

$$\delta = \frac{FL^3}{12EI_e} \tag{21}$$

The weak-axis moment of inertia of the equivalent beam is

$$I_e = \frac{\alpha d t^3}{12} = \frac{dt^3}{48} \tag{22}$$

Substituting Equations 17 and 22 into Equation 21 results in

$$\delta = \frac{6T_w L^3}{Ed^2 t^3} \tag{23}$$

Using the geometry in Figure 5, the rotation is

$$\theta_w = \frac{2\delta}{d} = \frac{12T_w}{E}\left(\frac{L}{dt}\right)^3 = \frac{T_w L^3}{12EC_w} \tag{24}$$

Substituting Equations 19 and 22 into Equation 21 results in the yield deflection

$$\delta_y = \frac{F_y L^2}{3Et} \tag{25}$$

The yield rotation is

$$\theta_{wy} = \frac{2\delta_y}{d} = \frac{2F_y L^2}{3Edt} \tag{26}$$

Finite element models of rectangular members subjected to torsion (May and Al-Shaarbaf, 1989; Baba and Kajita, 1982; Bathe and Chaudhary, 1982) exhibited an inelastic

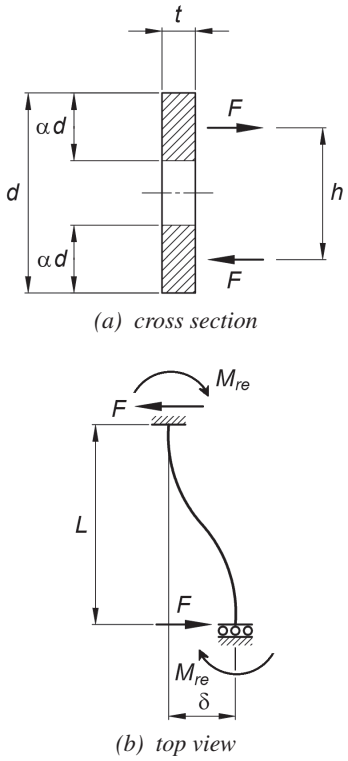

Fig. 4. Isolated flange method for warping analysis.

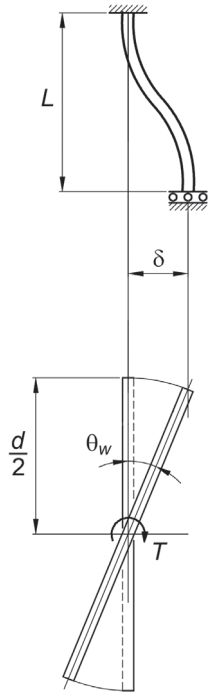

Fig. 5. Isolated flange method for warping rotation.

warping response similar to the uniform torsion curve in Figure 1, with the inelastic warping torsion contributing significantly to the total torsional resistance. For calculating the inelastic strength, F is assumed to act at the center of the effective depth, αd. The out-of-plane forces are

$$F = \frac{T_w}{h} = \frac{T_w}{d(1-\alpha)} \tag{27}$$

The weak-axis plastic flexural strength of the equivalent beam is

$$M_{pe} = \frac{F_y \alpha d t^2}{4} \tag{28}$$

Setting Equation 16 equal to Equation 28 and solving for F results in the out-of-plane force required for the plastic strength.

$$F_{wy} = \frac{F_y \alpha d t^2}{2L} \tag{29}$$

Setting Equation 27 equal to Equation 29 and solving for T_w results in the inelastic warping resistance.

$$T_{wp} = \frac{F_y d^2 t^2}{2L} \alpha(1-\alpha) \tag{30}$$

At $\alpha = ½$, the plastic warping strength, shown in Figure 2(c), is

$$T_{wp} = \frac{F_y d^2 t^2}{8L} \tag{31}$$

Comparing Equation 31 to Equation 20 shows that the plastic warping strength is 2.25 times the first-yield moment. However, the condition used to derive Equation 31 cannot be reached due to out-of-plane translation compatibility requirements at the member mid-depth. At $\alpha = 0.2113$, the plastic strength is reached only at the top and bottom fibers of the cross section, resulting in an inelastic warping strength of

$$T_{wi} = \frac{F_y d^2 t^2}{12L} \tag{32}$$

where

F = horizontal couple force, kips
I = moment of inertia, in.^{4}
T_w = warping torsional moment, kip-in.
αd = effective depth of the equivalent cross section, in.
δ = deflection of equivalent beam, in.
δ_y = yield deflection of equivalent beam, in.

THE WAGNER EFFECT

Also neglected in the design of torsion members is the Wagner effect (Wagner, 1936), which is a nonlinear, second-order torque that increases the torsional strength and stiffness (Kjar, 1967; Gregory, 1960). The Wagner torque is negligible for many connection geometries at practical serviceability rotations. However, a discussion is merited because the Wagner torsion contributes to the stable inelastic torsion-rotation curves exhibited by extended single-plate connection tests and finite element models. Also, the Wagner effect may explain why short connection elements, such as conventional single-plate connections, are only rarely limited by torsional rotations.

Elastic Strength

The Wagner solution for rectangular members was documented by Timoshenko (1956) and later by Cook and Young (1985) and Trahair (2003). Rotation of the member causes a longitudinal elongation of the fibers that are farthest from the center of rotation. Figure 6 shows that the tensile stresses caused by the elongation exerts a resisting torque about the

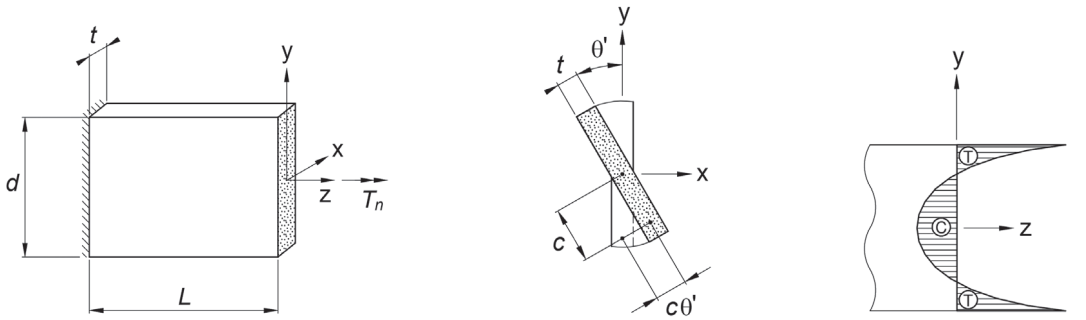

(a) torsionally loaded member *(b) cross section* *(c) longitudinal stresses*

Fig. 6. Mechanics of the Wagner effect.

axis of twist that increases with θ. The Wagner torsion is (Trahair, 2003)

$$T_n = \frac{EI_n}{2}(\theta')^3 \tag{33}$$

The Wagner constant is

$$I_n = \frac{d^5 t}{180} \tag{34}$$

Geometrically nonlinear elastic finite element models showed the accuracy of Equations 33 and 34 (Trahair, 2003). The axial stress developed by the Wagner effect, as shown in Figure 6(c), is (Cook and Young, 1985)

$$\sigma_n = \frac{E(\theta')^2}{2}\left(c^2 - \frac{d^2}{12}\right) \tag{35}$$

The maximum stress is located at the top and bottom edges of the member, where $c = d/2$

$$\sigma_{nt} = \frac{Ed^2(\theta')^2}{12} \tag{36}$$

If warping is neglected, the torsional resistance is the sum of the Wagner torsion and the uniform torsion (Cook and Young, 1985), resulting in

$$\begin{aligned} T_e &= T_u + T_n \\ &= \frac{Gdt^3\theta'}{3} + \frac{Ed^5 t(\theta')^3}{360} \\ &= \beta T_u \end{aligned} \tag{37}$$

and β is the normalized increase in torsional resistance due to the Wagner effect

$$\beta = 1 + \frac{Ed^4(\theta')^2}{120Gt^2} \tag{38}$$

For uniform members with constant torque along the length, $\theta' = \theta/L$ and the normalized increase in torsional resistance due to the Wagner effect is

$$\beta = 1 + \frac{Ed^4}{120G}\left(\frac{\theta}{tL}\right)^2 \tag{39}$$

where

I_n = Wagner constant, in.^{6}

T_n = Wagner torsional moment, kip-in.

c = distance to outermost fiber, in.

Evaluation of Equation 39 indicates that the torsional resistance is dependent on the rotation angle and can increase significantly with member depth. The Wagner torsion decreases with length and thickness.

Due to the short length of conventional single-plate shear connections, the Wagner effect can be significant. Figure 7(a) plots the torsion-rotation curve for a ⅜-in. × 18-in. plate, showing the uniform torsion, Wagner torsion, and the total torsional resistance. The plate is 3 in. long, which is the typical distance between the bolt line and the weld line for a conventional single-plate shear connection. The Wagner torsion is negligible for θ < 0.5° but is significant at 1° and provides a 220% increase in torsional resistance at θ = 2°. However, at θ = 2°, the maximum tensile stress is 106 ksi. For F_y = 50 ksi, first yield due to normal stress occurs at θ = 1.37°, where the increase in torsional resistance is 100%. For four different plate geometries, β is plotted in Figure 7(b) as a function of θ, where the substantial effect of decreasing the plate depth is clear.

Because extended single-plate shear connections are longer, and usually thicker, than conventional single-plate shear connections, the Wagner effect is often negligible for extended configurations. Figure 8(a) is a plot of the torsion-rotation curve for a ¾-in. × 18-in. plate, showing the uniform torsion, Wagner torsion and the total torsional resistance. The plate is 10 in. long, representing a common distance between the bolt line and the weld line for an extended single-plate shear connection. The Wagner torsion is negligible for the practical range of serviceability rotations, providing only 11% of the total torsion at θ = 3°. For four different plate geometries, β is plotted in Figure 8(b) as a function of θ, where the Wagner effect is shown to be significant only for plates with high depth-to-thickness ratios.

COMBINING TORSIONAL EFFECTS

The elastic torsional resistance is the sum of the uniform torsion, the warping torsion, and the Wagner torsion. However, because each torsional component contributes to the total resistance based on its relative stiffness, only one of the three components is likely to contribute its full first-yield torsional moment. In the elastic range, uniform and warping torsion can be combined using a stiffness analysis according to AISC Design Guide 9. This approach is preferred for member design, where beams are usually controlled by torsional rotation serviceability limits. However, designs that are based on a first-yield criterion underestimate the strength of connection elements.

Rotation

According to Trahair et al. (2008), the angle of rotation calculated for both uniform torsion and warping torsion can be calculated independently and combined using Equation 40 to estimate the actual angle of rotation.

$$\theta = \frac{\theta_u \theta_w}{\theta_u + \theta_w} \tag{40}$$

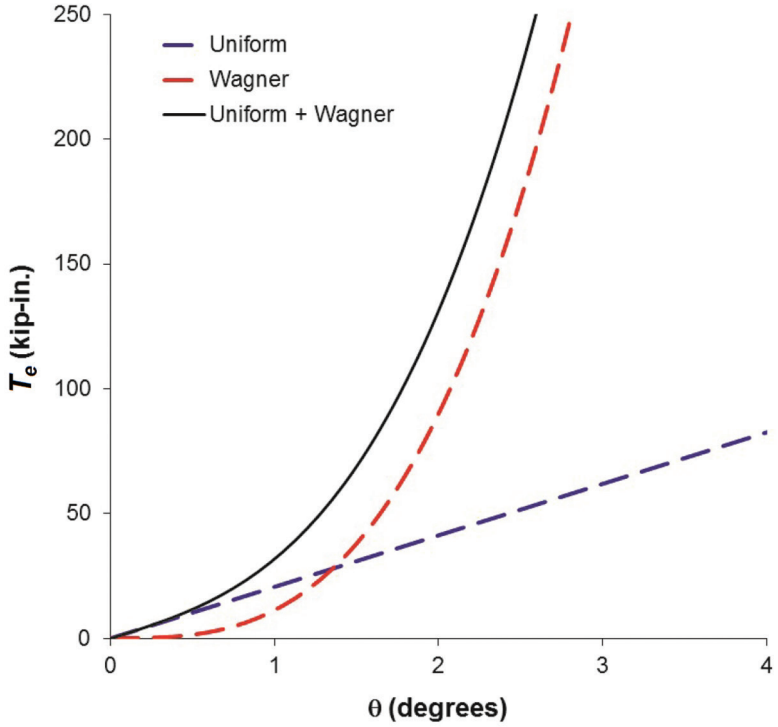

(a) T_e versus θ for a ⅜×18×3-in.-long plate

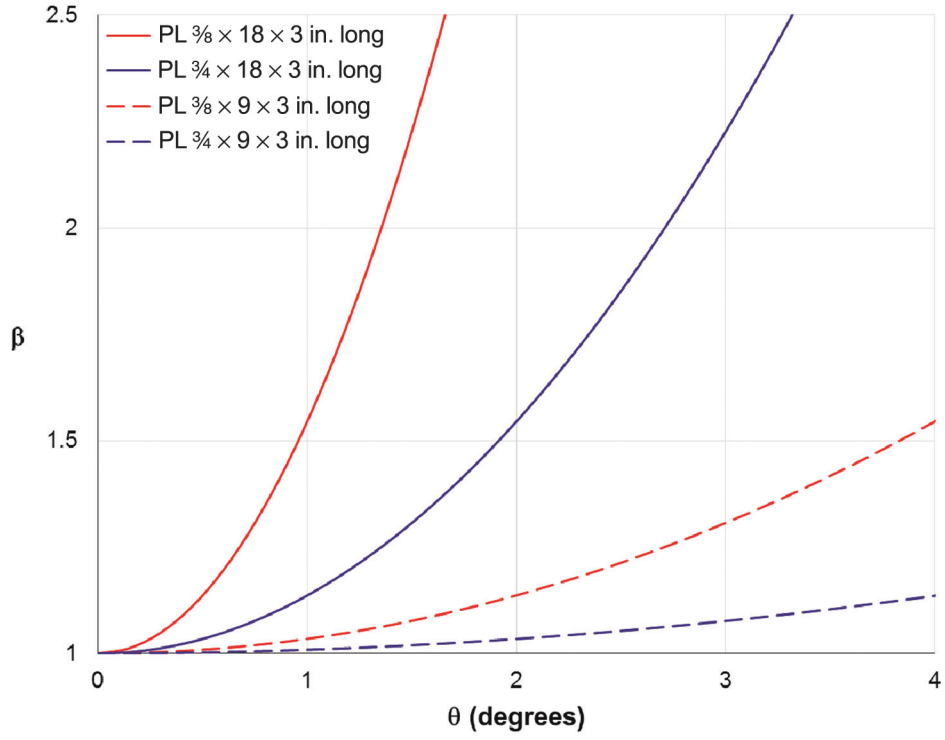

(b) β versus θ

Fig. 7. The Wagner effect for conventional single-plate shear connections.

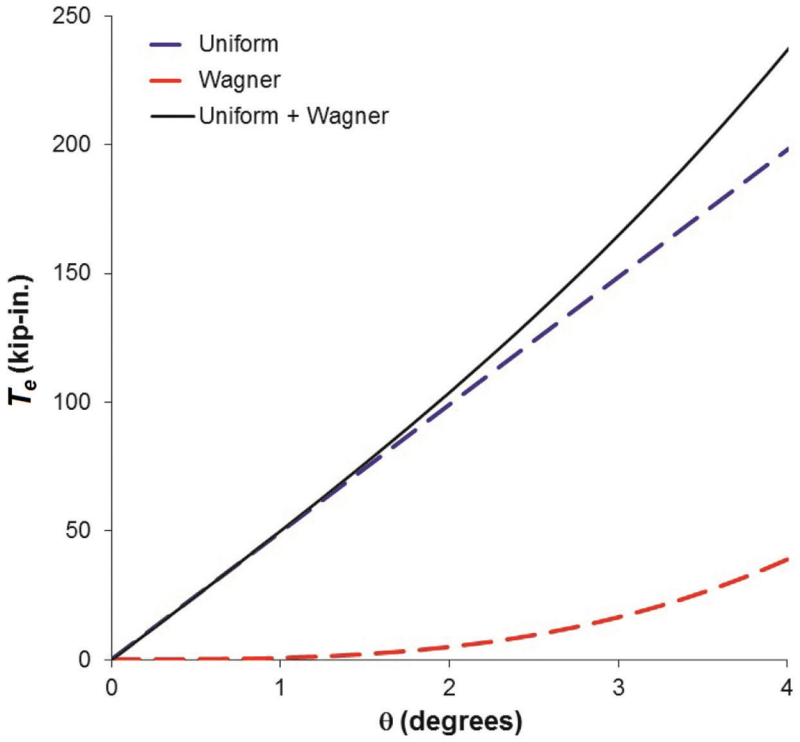

(a) T_e *versus* θ *for a ¾×18×10-in.-long plate*

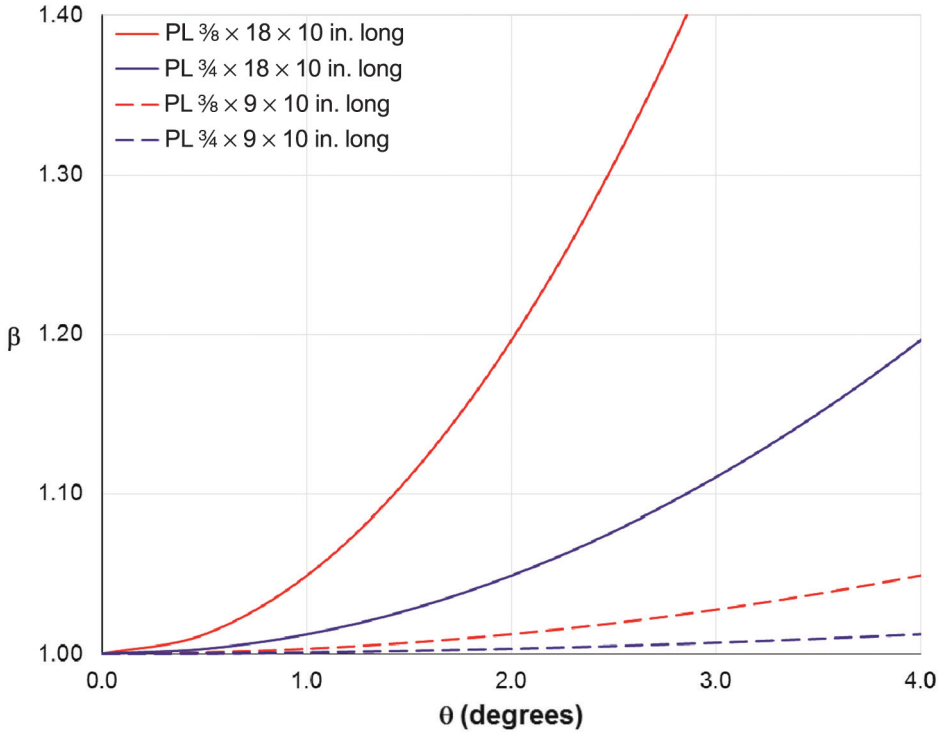

(b) β *versus* θ

Fig. 8. The Wagner effect for extended single-plate shear connections.

For members in the inelastic range, the angle of rotation can be estimated with Equation 41 (Pi and Trahair, 1994).

$$\theta_i = \frac{\theta}{1 - \frac{T_r}{2T_p}} \tag{41}$$

where

T_p = plastic torsional moment, kip-in.
T_r = required torsional moment, kip-in.
θ_u = angle of rotation for uniform torsion, rad
θ_w = angle of rotation for warping, rad

Plastic Strength

Because the Wagner effect requires large rotations for significant torsional resistance and the behavior under inelastic conditions is unclear, the Wagner torsion will be neglected. Dinno and Merchant (1965) and Pi and Trahair (1995) proposed a plastic torsion analysis where the plastic uniform torsion and the plastic warping torsion are evaluated independently and then added together to determine the total torsional resistance. This method assumes no interaction between uniform and warping torsion, which agrees well with experimental results on small-scale I-shaped members documented by Dinno and Merchant. Using the interaction suggested by Dinno and Merchant, the plastic torsional strength is

$$T_p = T_{up} + T_{wp} = T_{up}\left(1 + \frac{d}{2.4L}\right) \tag{42}$$

where

T_{up} = plastic uniform torsional moment, kip-in.
T_{wp} = plastic warping torsional moment, kip-in.

Figure 9 shows the predicted inelastic torsion versus rotation curves for a ¾×18×10-in.-long ASTM A572 Grade 50 plate. To show the effect of warping, both the uniform torsion curve and the uniform plus warping curves are plotted. The dashed lines show the elastic response and the solid lines show the inelastic curves. For the uniform torsion curve, the first-yield torsion is 101 kip-in. at $\theta = 2.05°$, and 96% of the plastic strength is developed at $\theta = 6.14°$. When warping is included, yielding is caused by warping normal stresses at a torsion of 72.7 kip-in. at $\theta = 0.447°$. However, the inelastic warping response shows a dramatic increase in stiffness and inelastic strength compared to the uniform torsion curve.

COMBINING TORSION WITH OTHER LOADS

Members subjected to both flexure and torsion must consider second-order effects and the strength reduction due to load interaction. After the required flexural and second-order torsional moments are determined, the available strength is calculated by combining the load ratios in an interaction equation.

Plastic Strength

Dowswell (2015) proposed Equation 43 for the interaction of flexure, shear, axial and torsion; however, the torsional interaction term was developed for uniform torsion and does not include the effects of warping and Wagner torsion. Because

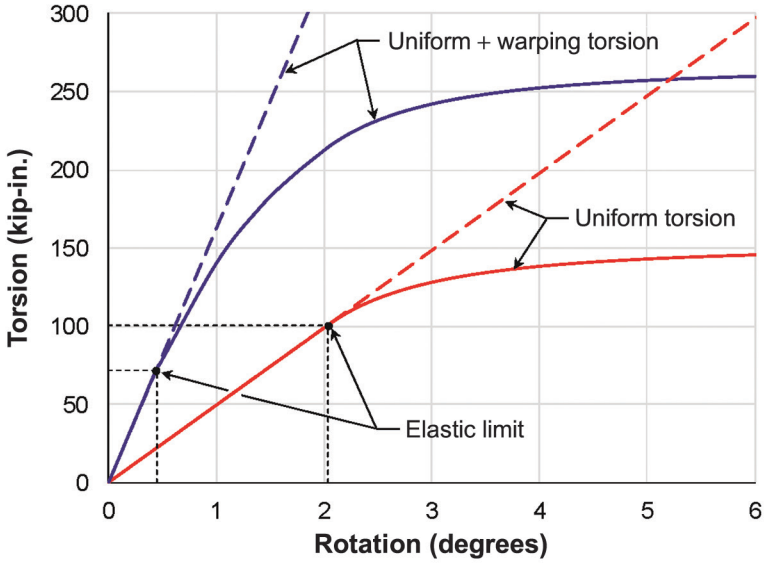

Fig. 9. Torsion-rotation curves for a ¾×18×10-in.-long ASTM A572 Grade 50 plate.

both warping and Wagner torsion develop longitudinal normal stresses, the resulting stress distributions are similar to the axial and flexural stresses. However, separating the torsional components and combining them with the flexural and axial load ratios would lead to unnecessary complexity in the interaction equation. Furthermore, due to the lack of research in this area, the accuracy of such an equation could not be verified. For design purposes, it is believed that T_p, as calculated with Equation 42, can be used in the torsion ratio of Equation 43.

$$\left(\frac{P_r}{P_y}\right)^2+\left(\frac{T_r}{T_p}\right)^2+\left(\frac{V_r}{V_p}\right)^4+\left[\left(\frac{M_{rx}}{M_{px}}\right)^{1.7}+\left(\frac{M_{ry}}{M_{py}}\right)^{1.7}\right]^{0.59}=1.0 \tag{43}$$

where

M_{px} = plastic bending moment about the x-axis, kip-in.
M_{py} = plastic bending moment about the y-axis, kip-in.
M_{rx} = required x-axis flexural strength, kip-in.
M_{ry} = required y-axis flexural strength, kip-in.
P_r = required axial strength, kips
P_y = axial yield load, kips
V_p = plastic shear strength, kips
V_r = required shear strength, kips

Second-Order Effects

For open sections subjected to both torsion and strong-axis flexure, the second-order torsional effects are dependent on the critical lateral-torsional buckling moment. Second-order torsional moments and rotations can be calculated by amplifying the results of a first-order analysis (Ashkinadze, 2008; Lindner and Glitsch, 2005; Boissonnade et al., 2002; Trahair and Teh, 2000; Pi and Trahair, 1994; Pastor, 1977). The amplification factor for rectangular members is (Zahn, 1984)

$$B=\frac{1}{1-\left(\frac{M_{rx}}{M_{cr}}\right)^2} \tag{44}$$

The second-order torsional rotation is

$$\theta_2=B\theta_1 \tag{45}$$

The second-order torsional moment is

$$T_2=BT_1 \tag{46}$$

The critical moment used in Equation 44 is

$$M_{cr}=F_{cr}S_x \tag{47}$$

The critical stress is calculated with AISC *Specification* (AISC, 2016) Equation F11–4

$$F_{cr}=\frac{1.9Et^2C_b}{Ld} \tag{48}$$

where

C_b = lateral-torsional buckling modification factor
F_{cr} = critical stress, ksi
M_{cr} = elastic critical buckling moment for strong-axis flexure, kip-in.
S_x = elastic section modulus about the x-axis, in.^{3}
T_1 = first-order torsional moment, kip-in.
θ_1 = first-order torsional rotation, rad

SINGLE-PLATE SHEAR CONNECTIONS

Single-plate shear connections, where the beam is field-bolted to a connecting plate as shown in Figure 10, have an

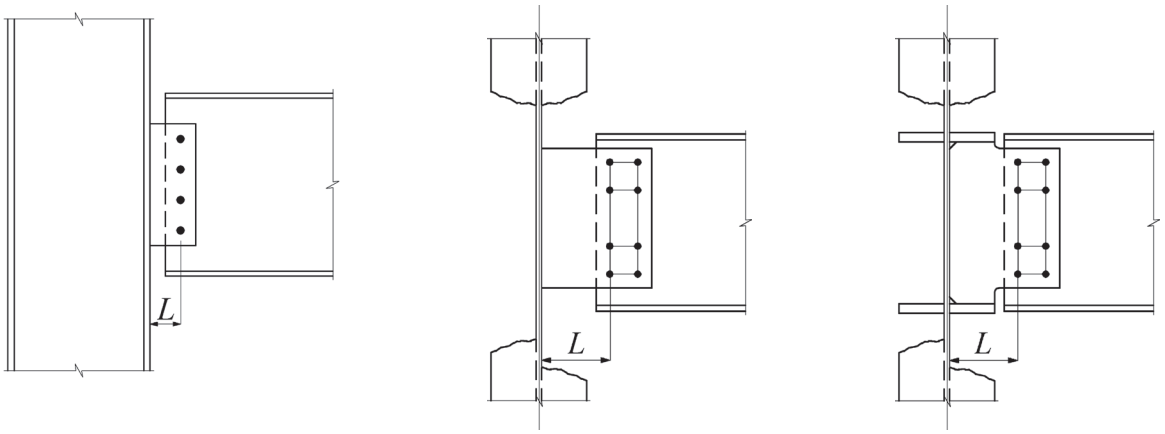

(a) conventional *(b) extended with no stiffener* *(c) extended with stiffener*

Fig. 10. Single-plate connections.

out-of-plane eccentricity between the beam and the plate. Under shear loading, this eccentricity causes a torsional moment, which has been previously discussed by Muir and Hewitt (2009) and Thornton and Fortney (2011).

Conventional Configuration

Of the many experimental research projects studying the behavior of conventional single-plate connections [Figure 10(a)], only the results of Moore and Owens (1992) showed significant torsional rotations. In these, and the remaining tests, the out-of-plane eccentricity had a negligible effect on the serviceability and strength and was not considered by the researchers as a significant design parameter. As discussed in previous sections of this paper, the conventional single-plate geometry maximizes the torsional resistance provided by warping and the Wagner effect.

Extended Configuration

Nonstiffened and stiffened extended single-plate shear connections are shown in Figures 10(b) and 10(c), respectively. Twisting of extended single-plate connections subjected to shear loading has been reported in experimental specimens (Sherman and Ghorbanpoor, 2002) and finite element models (Hijaj and Mahamid, 2017; Abou-Zidan, 2014; Suleiman, 2013). The experimental measurements of Goodrich (2005) and Sherman and Ghorbanpoor (2002) showed an increase in torsional strength and rotational stiffness when the plate is welded to a stiffener. The finite element models of Rahman et al. (2007) and Mahamid et al. (2007) showed similar results.

For nonstiffened connections, the design procedure in the AISC *Steel Construction Manual* (AISC, 2017) was developed by Muir and Hewitt (2009). The equations implicitly limit excessive torsional rotations by combining the shear and flexural strengths using an elliptical interaction to approximate von Mises theory. If the torsional loads are explicitly included in the calculations, the load ratios can be combined using plastic interaction according to Equation 49, which is simplified from Equation 43.

$$\frac{M_{rx}}{M_{nx}}+\left(\frac{T_2}{T_p}\right)^2+\left(\frac{R_r}{V_p}\right)^4=1.0 \tag{49}$$

The total plastic torsional strength, T_p, is calculated with Equations 7, 31 and 42. The second-order torsional moment is calculated with Equations 44 and 46, and the first-order torsional moment is

$$T_1=R_r e \tag{50}$$

The eccentricity is

$$e=\frac{t+t_w}{2} \tag{51}$$

The strong-axis flexural moment, M_{rx}, is dependent on the location of the inflection point. At flexible supports, it is conservative to assume the connection behaves as a frictionless pin, resulting in

$$M_{rx}=R_r L \tag{52}$$

The plastic shear strength is

$$V_p=0.6F_y td \tag{53}$$

where

M_{nx} = strong-axis flexural strength, kip-in.
R_r = required beam end shear reaction, kips
T_2 = second-order torsional moment, kip-in.
e = horizontal eccentricity for a single-plate connection, in.
t = plate thickness, in.
t_w = beam web thickness, in.

The strong-axis flexural strength, M_{nx}, can be calculated according to AISC *Specification* Section F11, with $C_b = 1.84$ when the beam is braced near the end and $C_b = 1.26$ when the beam is unbraced near the end (Dowswell, 2004). These C_b factors are also used in Equation 48 to calculate the critical stress for the second-order torsion amplifier.

The plastic strength according to the equations in this section are compared to the available experimental and finite element results in Table 1. Only nonstiffened specimens with no beam bracing near the connection were considered. The four specimens listed failed by excessive twisting of the plate. R_c is the shear strength calculated with the actual dimensions and yield strengths, R_e is the approximate experimental shear load where the load-deflection curve became nonlinear, and R_u is the maximum experimental shear load.

The last column of the table lists the test-to-calculated ultimate strength ratio, R_u/R_c, which has an average of 1.28 for the four specimens. Therefore, the plastic interaction equation is conservative, possibly because the Wagner effect and the effects of strain hardening were neglected. Because the calculations were based on the plastic strength, nonlinear behavior was expected at loads significantly below R_c; however, for two of the specimens, R_e/R_c is greater than 1.00.

Lateral Bracing

Thornton and Fortney (2011) derived a method to predict the torsional resistance of extended single-plate shear connections with a slab or deck attached to the beam top flange. For torsional resistance, the method utilizes both the uniform torsion strength of the plate and the torsional resistance provided by the slab/deck flexural strength. A design method has not been established for the case where the beam top flange is restrained against lateral translation, but not rotation. The equations presented in this section rely only on the lateral resistance of the beam bracing.

Table 1. Nonstiffened Single-Plate Connections											
Reference	Spec. No.	t (in.)	d (in.)	t_w (in.)	L (in.)	F_y (ksi)	R_c (kips)	R_e (kips)	R_u (kips)	R_e/R_c	R_u/R_c
Sherman and Ghorbanpoor (2002)	2U	0.371	15.00	0.495	6.30	42.6	71.4	65	82.9	0.910	1.16
	4U	0.495	15.00	0.495	10.0	43.5	77.7	82	98.7	1.06	1.27
	6UB	0.495	18.00	0.650	10.0	43.5	96.0	119	136	1.24	1.42
Abou-Zidan (2014)	15	0.394	9.05	0.382	6.38	50.8	43.7	36	55.1	0.82	1.26

R_c = calculated shear strength, kips
R_e = the approximate experimental shear load where the load-deflection curve became nonlinear, kips
R_u = the maximum experimental shear load, kips

When lateral bracing is present at both the top and bottom flanges [Figure 11(a)], the eccentric torsion can be resisted completely by the braces. Finite element models by Abou-Zidan (2014) and Suleiman (2013) showed that top-flange lateral bracing near the beam end significantly increases the torsional resistance of extended single-plate shear connections. For cases where only top-flange bracing is present, a portion of the eccentric torsion can be resisted with a couple between the brace and the centroid of the plate [Figure 11(b)].

$$T_b = Fh \tag{54}$$

Assuming the plate deforms in double-curvature, as shown in Figure 4(b), the required weak-axis moment at each end of the plate is

$$M_{ry} = \frac{FL}{2} \tag{55}$$

The resisting moment of the plate is

$$M_{py} = F_y \frac{dt^2}{4} \tag{56}$$

Setting $M_{ry} = M_{py}$, solving for F, and substituting into Equation 54 results in a torsional resistance of

$$T_b = F_y \frac{hdt^2}{2L} \tag{57}$$

T_b can be combined with the uniform torsion strength to get the total torsional resistance.

$$T_p = T_{up} + T_b = T_{up}\left(1 + \frac{5h}{3L}\right) \tag{58}$$

where

T_b = torsional resistance provided by a top flange lateral brace, kip-in.

h = distance between couple forces, F, in.

Although no interaction is assumed between the two torsional components, Equation 58 is believed to be adequate for design purposes. The available information on flexure-torsion interaction of rectangular members was summarized by Dowswell (2015); however, the interaction of torsion with other loads is not well understood. For example, the theory

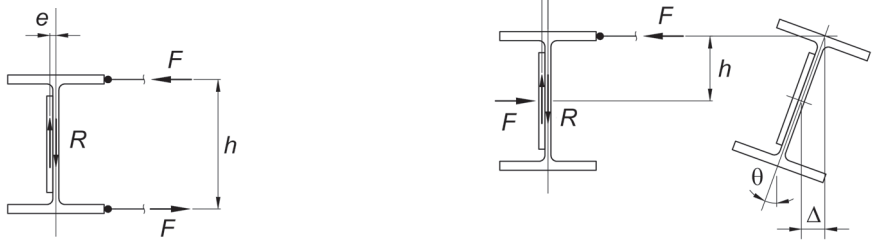

(a) lateral bracing at top and bottom flanges *(b) lateral bracing at top flange*

Fig. 11. Torsional rotation at braced beam ends.

Table 2. Nonstiffened Single-Plate Connections with Top-Flange Lateral Bracing											
Spec. No.	Failure Mode	t (in.)	d (in.)	t_w (in.)	L (in.)	F_y (ksi)	R_c (kips)	R_e (kips)	R_u (kips)	R_e/R_c	R_u/R_c
11	Yielding	0.236	9.05	0.382	6.38	50.8	28.5	39	61.8	1.37	2.17
13	Twisting	0.394	9.05	0.382	6.38	50.8	54.6	56	94.4	1.03	1.73

R_c = calculated shear strength, kips
R_e = the approximate experimental shear load where the load-deflection curve became nonlinear, kips
R_u = the maximum experimental shear load, kips

and experiments of Neal (1950) and Witrick (1952) showed that the torsional stiffness remains at its elastic value after the member has yielded in flexure. For single-plate connections, contrasting results were obtained by Suleiman (2013), where nonlinear torsional behavior initiated at loads well below the corresponding yield loads based on the vertical shear-deformation curves (Figure 12). Additionally, the research summarized by Dowswell (2015) showed that Equation 49 is conservative for flexure-torsion interaction. Furthermore, any reduction in load due to interaction is likely to be offset by neglecting the Wagner torsion and warping torsion.

Only one of the finite element models by Abou-Zidan (2014) failed due to excessive twisting. For another model, failure was caused by yielding of the plate between the weld line and the bolt line. For both of these specimens, T_p was calculated with Equation 58 and the torsion ratio was combined with the shear and flexure ratios according to Equation 49. The results are listed in Table 2, where it is shown that the equations are conservative. The last column of the table lists the test-to-calculated ultimate strength ratio, R_u/R_c, which is close to two for both specimens. With an average R_e/R_c ratio of 1.20, the proposed equations provide reasonable estimates of the load causing the onset of nonlinear behavior for both models.

Practical Results

This section shows the results of including torsion in the analysis of single plate connections. The discussions include connections with various configurations supporting a W18×35 beam, which has a web thickness, t_w, of 0.300 in. In all cases, the plate material is ASTM A572 Gr. 50 and the depth, d, is 15 in.

The first results are for a conventional single-plate shear connection, as shown in Figure 10(a), with a plate thickness of t = ⅜ in. and L = 3 in. The Wagner strength, calculated with Equation 33 at a rotation of 0.03 rad., is 22.9 kip-in. Adding this to the plastic torsional strength calculated with Equation 42 results in a plastic torsional resistance of 120 kip-in. The elastic uniform torsional resistance, T_{uy}, is 21.1 kip-in., which is only 18% of the plastic torsional resistance at 0.03 rad. Using Equation 49 to combine the flexural, torsional and shear loads results in a nominal shear strength of 149 kips. For a plate with 15⁄16-in.-diameter holes, the AISC *Manual* design procedure results in a nominal shear strength of 146 kips, which is controlled by the shear rupture limit state. Because plate yielding is a key component in the rotational ductility of these connections, the torsional stresses may actually enhance the performance. These results show why the common practice of neglecting torsion in the design of conventional single-plate shear connections is warranted.

The next results are for extended single-plate shear connections, as shown in Figure 10(b), with t = ⅝ in. and L = 9 in. Several bracing conditions were considered: Case 1, unbraced beam; Case 2, beam with top-flange lateral bracing near the connection; and Case 3, beam with torsional bracing near the connection. The AISC *Manual* design procedure results in a nominal shear strength of 161 kips;

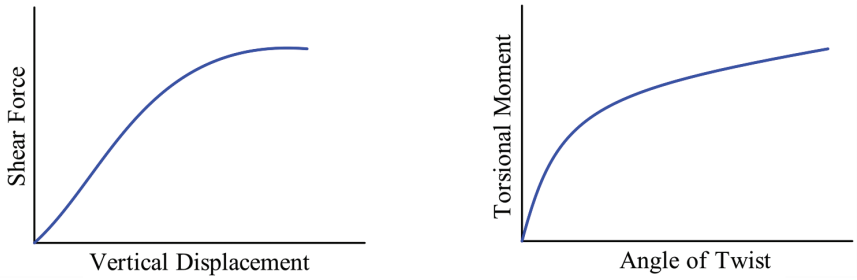

Fig. 12. Shear-displacement and torsion-rotation curves (Suleiman, 2013).

however, the results are valid only for beams with bracing located near the connection. In all cases, the Wagner torsion is neglected and load interaction is calculated according to Equation 49. The elastic uniform torsional resistance is 93.8 kip-in.

Case 1: Because beam bracing is not provided near the connection, the AISC *Manual* design procedure is not applicable. Also, this configuration can significantly reduce the lateral-torsional buckling strength of the beam. The plastic torsional strength calculated with Equation 42 is 202 kip-in., which is more than double the elastic uniform torsional resistance. The second-order amplification factor and the buckling strength of the plate were calculated with $C_b = 1.26$. The calculations resulted in a shear strength of 151 kips, which is 6% less than the strength calculated with the AISC *Manual* design procedure.

Case 2: For this case, the plastic torsional strength can be calculated using either Equation 42 or Equation 58. The plastic torsional strength calculated with Equation 42 is the same as for Case 1. The plastic torsional strength calculated with Equation 58 is 285 kip-in., which is three times the elastic uniform torsional resistance. The second-order amplification factor and the buckling strength of the plate were calculated with $C_b = 1.84$. The calculations resulted in shear strengths of 153 kips and 161 kips when using Equation 42 and Equation 58, respectively. In both cases, the result is within 5% of the strength calculated with the AISC *Manual* design procedure.

Case 3: For this case, the torsion is resisted by the beam bracing system and $T_2 = 0$, resulting in a shear strength of 170 kips. This is 6% greater than the strength calculated with the AISC *Manual* design procedure.

PROPOSED DESIGN METHOD

The design process can be simplified by limiting the second-order amplification factor to 1.10 and solving for the minimum thickness required to reach the plastic flexural strength. Substituting $B = 1.10$ and $M_{rx} = \phi M_{px}$ into Equation 44, combining with Equations 47 and 48, and solving for t results in Equation 59.

$$t_{min} = 1.54\sqrt{\frac{LdF_y}{C_bE}} \tag{59}$$

where

C_b = 1.84 when the connection element is braced at both ends

= 1.26 when the connection element is braced only at one end

This minimum plate thickness also ensures that AISC *Specification* Section F11 will always result in $M_{nx} = M_{px}$ for $C_b \geq 1.07$. For $t \geq t_{min}$, the required second-order torsional moment is

$$T_r = 1.1T_1 \tag{60}$$

Based on the design recommendations of Dowswell (2016), Equation 43 can be used for design by modifying the exponent applied to the axial load ratio and substituting the available strengths for plastic strengths.

$$\left(\frac{P_r}{P_c}\right)^k + \left(\frac{T_r}{T_c}\right)^2 + \left(\frac{V_r}{V_c}\right)^4 + \left[\left(\frac{M_{rx}}{M_{cx}}\right)^{1.7} + \left(\frac{M_{ry}}{M_{cy}}\right)^{1.7}\right]^{0.59} = 1.0 \tag{61}$$

where

M_{cx} = available flexural strength about the x-axis, kip-in.
= ϕM_{px} (LRFD) or M_{px}/Ω (ASD)

M_{cy} = available flexural strength about the y-axis, kip-in.
= ϕM_{py} (LRFD) or M_{py}/Ω (ASD)

P_c = available axial strength calculated according to AISC *Specification* Section J4.1(a) or Section J4.4 for tension and compression elements, respectively, kips
= ϕP_n (LRFD) or P_n/Ω (ASD)

T_c = available torsional strength, kips
= ϕT_p (LRFD) or T_p/Ω (ASD)

V_c = available shear strength calculated according to AISC *Specification* Section J4.2(a), kips
= ϕV_n (LRFD) or V_n/Ω (ASD)

k = 1 for compression loads
= 2 for tensile loads

For connection elements that are braced only at one end and free at the other end, the nominal plastic torsional strength, T_p, is calculated with Equation 42. For extended single-plate shear connections with beam top flange lateral bracing near the connection, T_p can be calculated with Equation 58. For extended single-plate shear connections with beam lateral and torsional bracing near the connection, the torsional load at the plate can be neglected ($T_r = 0$).

DESIGN EXAMPLES

Example 1

Given

In this example, a W21×111 beam is connected to a column web with an extended single-plate connection, as shown in Figure 13. The beam is not braced, but the effect of the connection on the lateral-torsional buckling strength has been considered in the beam design. The connection is subjected to an axial tension force, P, a vertical shear force, R, and a horizontal out-of-plane force, F. The plate is ¾-in. × 15-in. ASTM A572 Grade 50.

The vertical and horizontal forces are:

LRFD	ASD
$P_u = 30$ kips $R_u = 60$ kips $F_u = 6$ kips	$P_a = 20$ kips $R_a = 40$ kips $F_a = 4$ kips

Solution

A572 Gr. 50: $F_y = 50$ ksi
W18×50: $t_w = 0.550$ in.
Plate: $t = ¾$ in. $d = 15$ in. $L = 10$ in.
$C_b = 1.26$
$k = 2$

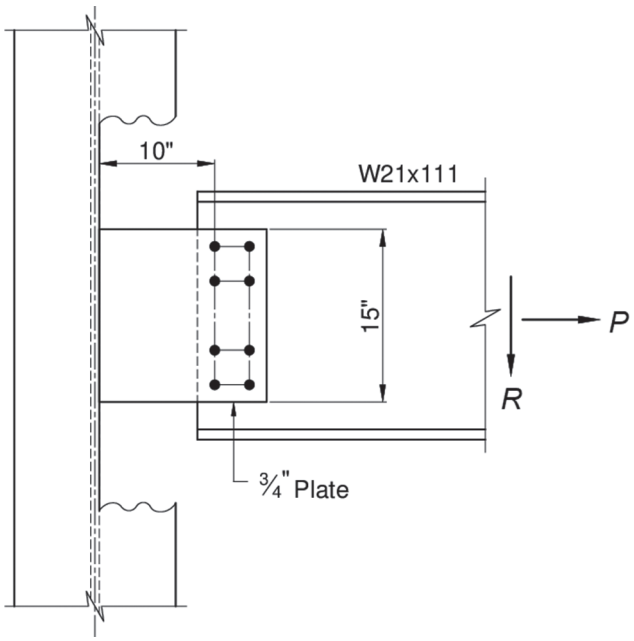

Fig. 13. Beam connection for Example 1.

The required minimum plate thickness calculated with Equation 59 is:

$$t_{min} = 1.54\sqrt{\frac{LdF_y}{C_bE}} \tag{59}$$

$$= 1.54\sqrt{\frac{(10 \text{ in.})(15 \text{ in.})(50 \text{ ksi})}{(1.26)(29{,}000 \text{ ksi})}}$$

$$= 0.698 \text{ in.} < 0.750 \text{ in.} \quad \textbf{o.k.}$$

Combining Equations 50, 51 and 60, the required torsional moment, T_r, is:

LRFD	ASD
$T_u = 1.1R_u\left(\frac{t+t_w}{2}\right)$	$T_a = 1.1R_a\left(\frac{t+t_w}{2}\right)$
$= (1.1)(60 \text{ kips})\left(\frac{0.550 \text{ in.} + 0.750 \text{ in.}}{2}\right)$	$= (1.1)(40 \text{ kips})\left(\frac{0.550 \text{ in.} + 0.750 \text{ in.}}{2}\right)$
$= 42.9$ kip-in.	$= 28.6$ kip-in.

The required shear force, V_r, is:

LRFD	ASD
$V_u = \sqrt{R_u^2 + F_u^2}$	$V_a = \sqrt{R_a^2 + F_a^2}$
$= \sqrt{(60 \text{ kips})^2 + (6 \text{ kips})^2}$	$= \sqrt{(40 \text{ kips})^2 + (4 \text{ kips})^2}$
$= 60.3$ kips	$= 40.2$ kips

The required strong-axis flexural strength, M_{rx}, is:

LRFD	ASD
$M_{ux} = (60 \text{ kips})(10 \text{ in.})$	$M_{ax} = (40 \text{ kips})(10 \text{ in.})$
$= 600$ kip-in.	$= 400$ kip-in.

The required weak-axis flexural strength, M_{ry}, is:

LRFD	ASD
$M_{uy} = (6 \text{ kips})(10 \text{ in.})$	$M_{ay} = (4 \text{ kips})(10 \text{ in.})$
$= 60.0$ kip-in.	$= 40.0$ kip-in.

The nominal axial tensile strength is:

$$P_n = (50 \text{ ksi})(0.750 \text{ in.})(15 \text{ in.})$$
$$= 563 \text{ kips}$$

The available axial tensile strength is:

LRFD	ASD
$\phi P_n = (0.90)(563 \text{ kips})$	$P_n/\Omega = 563 \text{ kips}/1.67$
$= 507$ kips	$= 337$ kips

Combining Equations 7 and 42, the nominal torsional strength is:

$$T_p = \frac{(0.6)(50\text{ ksi})(0.750\text{ in.})^2(15\text{ in.})}{2}\left[1+\frac{15\text{ in.}}{(2.4)(10\text{ in.})}\right]$$
$$= 185\text{ kip-in.}$$

The available torsional strength is:

LRFD	ASD
$\phi T_p = (0.90)(185\text{ kip-in.})$ $= 167\text{ kip-in.}$	$T_p/\Omega = 185\text{ kip-in.}/1.67$ $= 111\text{ kips}$

The nominal shear strength is:

$$V_n = (0.6)(50\text{ ksi})(0.750\text{ in.})(15\text{ in.})$$
$$= 338\text{ kips}$$

The available shear strength is:

LRFD	ASD
$\phi V_n = (1.00)(338\text{ kips})$ $= 338\text{ kips}$	$V_n/\Omega = 338\text{ kips}/1.50$ $= 225\text{ kips}$

The nominal strong-axis flexural strength is:

$$M_{nx} = (50\text{ ksi})\left[\frac{(0.750\text{ in.})(15\text{ in.})^2}{4}\right]$$
$$= 2{,}110\text{ kip-in.}$$

The available strong-axis flexural strength is:

LRFD	ASD
$\phi M_{nx} = (0.90)(2{,}110\text{ kip-in.})$ $= 1{,}900\text{ kip-in.}$	$M_{nx}/\Omega = 2{,}110\text{ kip-in.}/1.67$ $= 1{,}260\text{ kip-in.}$

The nominal weak-axis flexural strength is:

$$M_{ny} = (50\text{ ksi})\left[\frac{(15\text{ in.})(0.750\text{ in.})^2}{4}\right]$$
$$= 105\text{ kip-in.}$$

The available weak-axis flexural strength is:

LRFD	ASD
$\phi M_{ny} = (0.90)(105\text{ kip-in.})$ $= 94.5\text{ kip-in.}$	$M_{ny}/\Omega = 105\text{ kip-in.}/1.67$ $= 62.9\text{ kip-in.}$

For LRFD, interaction according to Equation 61 is:

$$\left(\frac{30\text{ kips}}{507\text{ kips}}\right)^2+\left(\frac{42.9\text{ kip-in.}}{167\text{ kip-in.}}\right)^2+\left(\frac{60.3\text{ kips}}{338\text{ kips}}\right)^4+\left[\left(\frac{600\text{ kip-in.}}{1{,}900\text{ kip-in.}}\right)^{1.7}+\left(\frac{60.0\text{ kip-in.}}{94.5\text{ kip-in.}}\right)^{1.7}\right]^{0.59} \quad (61)$$

$$=0.812<1.0 \quad \textbf{o.k.}$$

For ASD, interaction according to Equation 61 is:

$$\left(\frac{20\text{ kips}}{337\text{ kips}}\right)^2+\left(\frac{28.6\text{ kip-in.}}{111\text{ kip-in.}}\right)^2+\left(\frac{40.2\text{ kips}}{225\text{ kips}}\right)^4+\left[\left(\frac{400\text{ kip-in.}}{1{,}260\text{ kip-in.}}\right)^{1.7}+\left(\frac{40.0\text{ kip-in.}}{62.9\text{ kip-in.}}\right)^{1.7}\right]^{0.59} \quad (61)$$

$$=0.815<1.0 \quad \textbf{o.k.}$$

Example 2

Given

During erection of the W21 beam in Example 1, a field correction requires the beam to be moved ½ in. horizontally, perpendicular to the beam axis. If a ½-in. filler plate is installed between the ¾-in. plate and the beam web, is the plate strength adequate?

Solution

The eccentricity increases to:

$$e=\frac{0.550\text{ in.}+0.750\text{ in.}}{2}+0.500\text{ in.}$$

$$=1.15\text{ in.}$$

The required torsional moment, T_r, increases to:

LRFD	ASD
$T_u=(1.1)(60\text{ kips})(1.15\text{ in.})$ $=75.9\text{ kip-in.}$	$T_a=(1.1)(40\text{ kips})(1.15\text{ in.})$ $=50.6\text{ kip-in.}$

For LRFD, interaction according to Equation 61 is:

$$\left(\frac{30\text{ kips}}{507\text{ kips}}\right)^2+\left(\frac{75.9\text{ kip-in.}}{167\text{ kip-in.}}\right)^2+\left(\frac{60.3\text{ kips}}{338\text{ kips}}\right)^4+\left[\left(\frac{600\text{ kip-in.}}{1{,}900\text{ kip-in.}}\right)^{1.7}+\left(\frac{60.0\text{ kip-in.}}{94.5\text{ kip-in.}}\right)^{1.7}\right]^{0.59} \quad (61)$$

$$=0.953<1.0 \quad \textbf{o.k.}$$

For ASD, interaction according to Equation 61 is:

$$\left(\frac{20\text{ kips}}{337\text{ kips}}\right)^2+\left(\frac{50.6\text{ kip-in.}}{111\text{ kip-in.}}\right)^2+\left(\frac{40.2\text{ kips}}{225\text{ kips}}\right)^4+\left[\left(\frac{400\text{ kip-in.}}{1{,}260\text{ kip-in.}}\right)^{1.7}+\left(\frac{40.0\text{ kip-in.}}{62.9\text{ kip-in.}}\right)^{1.7}\right]^{0.59} \quad (61)$$

$$=0.956<1.0 \quad \textbf{o.k.}$$

Example 3

Given

In this example, a gusset plate connects a WT horizontal brace to a roof beam and a truss top chord. Figure 14 shows the connection rotated into the roof plane. Both the brace and the roof beam are in the roof plane, which is sloped at 20° from horizontal, and the chord web is in the horizontal plane. Because the chord is rotated 20° relative to the gusset plate, the gusset-to-chord interface has been detailed with a skewed end plate welded to the gusset plate. The end plate is 1-in. × 18-in. ASTM A572 Grade 50. The brace component parallel to the truss chord, P_L, is transferred into the chord, and the component perpendicular to the chord, P_T, is transferred into the roof beam. Because the bracing work point is located at the chord centroid, the chord was designed assuming concentric axial loading; therefore, P_L must be transferred to the work point at the chord centroid. For static equilibrium of the connection, the 1-in. end plate is subjected to both flexure and torsion. Only the end plate at the gusset-to-chord interface will be designed in this example.

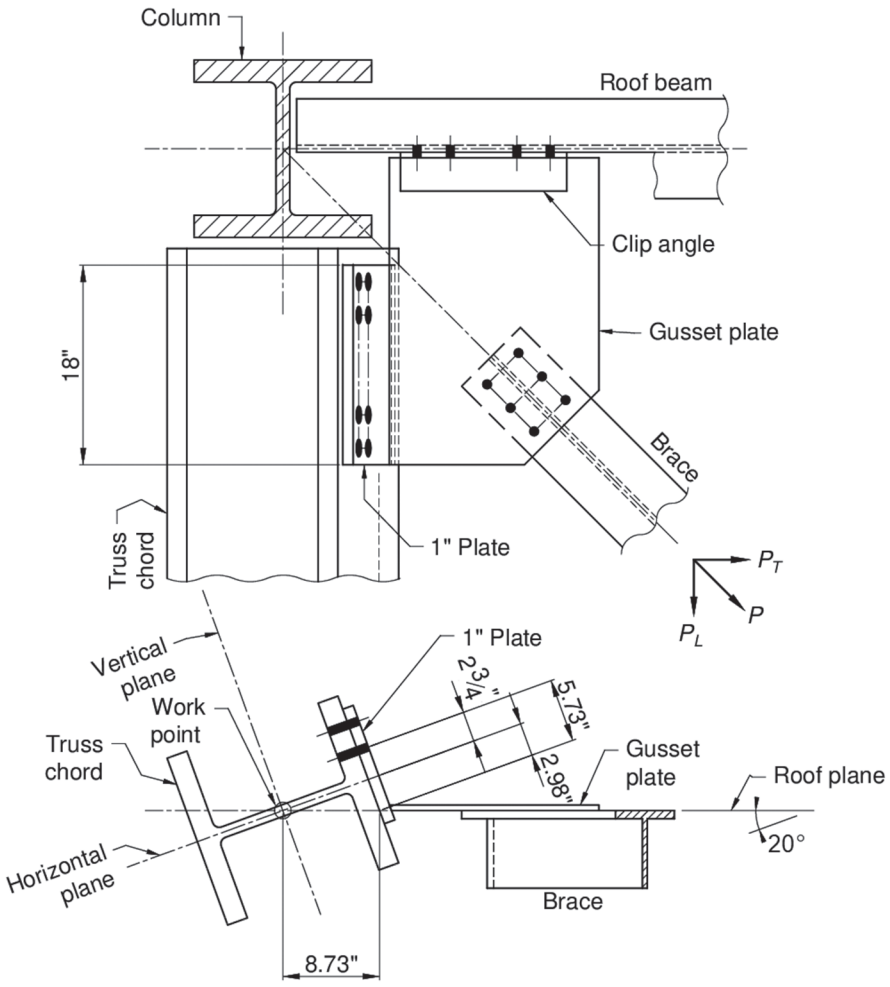

Fig. 14. Horizontal brace connection for Example 3.

Solution

The brace component parallel to the truss chord axis is:

LRFD	ASD
$P_{uL} = 50.0$ kips	$P_{aL} = 33.3$ kips

A572 Gr. 50: $F_y = 50$ ksi
Plate: $t = 1$ in. $d = 15$ in. $L = 5.73$ in.
$C_b = 1.84$

The required minimum plate thickness calculated with Equation 59 is:

$$t_{min} = 1.54\sqrt{\frac{LdF_y}{C_bE}} \tag{59}$$

$$= 1.54\sqrt{\frac{(5.73 \text{ in.})(15 \text{ in.})(50 \text{ ksi})}{(1.84)(29{,}000 \text{ ksi})}}$$

$$= 0.284 \text{ in.} < 1 \text{ in.} \quad \textbf{o.k.}$$

The moment in the roof plane is P_L multiplied by the eccentricity in the roof plane, which is the distance from the work point to the faying surface between the chord flange and the 1-in. end plate.

LRFD	ASD
$M_{ui} = (50 \text{ kips})(8.73 \text{ in.})$ $= 437$ kip-in.	$M_{ai} = (33.3 \text{ kips})(8.73 \text{ in.})$ $= 291$ kip-in.

The required strong-axis flexural strength of the end plate, M_{rx}, is:

LRFD	ASD
$M_{ux} = (437 \text{ kip-in.})\sin(20°)$ $= 149$ kip-in.	$M_{ax} = (291 \text{ kip-in.})\sin(20°)$ $= 99.5$ kip-in.

The first-order torsional moment in the end plate is:

LRFD	ASD
$T_{u1} = (437 \text{ kip-in.})\cos(20°)$ $= 411$ kip-in.	$T_{a1} = (291 \text{ kip-in.})\cos(20°)$ $= 273$ kip-in.

The required second-order torsional strength of the end plate, T_r, is:

LRFD	ASD
$T_u = (1.1)(411 \text{ kip-in.})$ $= 452$ kip-in.	$T_a = (1.1)(273 \text{ kip-in.})$ $= 300$ kip-in.

The required shear strength of the end plate, V_r, is:

LRFD	ASD
$V_u = P_{uL} = 50.0$ kips	$V_a = P_{aL} = 33.3$ kips

These loads are shown on the free-body diagram in Figure 15.

Combining Equations 7 and 42, the nominal torsional strength is:

$$T_p = \frac{(0.6)(50\text{ ksi})(1\text{ in.})^2(18\text{ in.})}{2}\left[1+\frac{18\text{ in.}}{(2.4)(5.73\text{ in.})}\right]$$
$$= 623\text{ kip-in.}$$

The available torsional strength is:

LRFD	ASD
$\phi T_p = (0.90)(623\text{ kip-in.})$ $= 561\text{ kip-in.}$	$T_p/\Omega = 623\text{ kip-in.}/1.67$ $= 373\text{ kips}$

The nominal shear strength is:

$$V_n = (0.6)(50\text{ ksi})(1\text{ in.})(18\text{ in.})$$
$$= 540\text{ kips}$$

The available shear strength is:

LRFD	ASD
$\phi V_n = (1.00)(540\text{ kips})$ $= 540\text{ kips}$	$V_n/\Omega = 540\text{ kips}/1.50$ $= 360\text{ kips}$

The nominal strong-axis flexural strength is:

$$M_{nx} = (50\text{ ksi})\left[\frac{(1\text{ in.})(18\text{ in.})^2}{4}\right]$$
$$= 4{,}050\text{ kip-in.}$$

The available strong-axis flexural strength is:

LRFD	ASD
$\phi M_{nx} = (0.90)(4{,}050\text{ kip-in.})$ $= 3{,}650\text{ kip-in.}$	$M_{nx}/\Omega = 4{,}050\text{ kip-in.}/1.67$ $= 2{,}430\text{ kip-in.}$

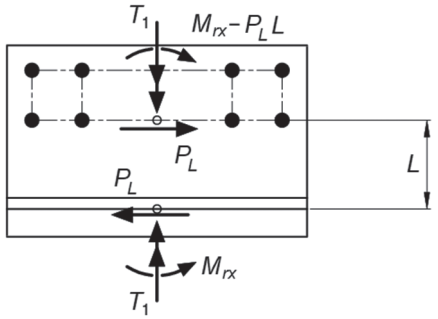

Fig. 15. Free-body diagram of 1-in. end plate.

For LRFD, interaction according to Equation 61 is:

$$\left(\frac{452 \text{ kip-in.}}{561 \text{ kip-in.}}\right)^2+\left(\frac{50.0 \text{ kips}}{540 \text{ kips}}\right)^4+\frac{149 \text{ kip-in.}}{3{,}650 \text{ kip-in.}} \tag{61}$$
$$= 0.690 < 1.0 \quad \textbf{o.k.}$$

For ASD, interaction according to Equation 61 is:

$$\left(\frac{300 \text{ kip-in.}}{373 \text{ kip-in.}}\right)^2+\left(\frac{33.3 \text{ kips}}{360 \text{ kips}}\right)^4+\frac{99.5 \text{ kip-in.}}{2{,}430 \text{ kip-in.}} \tag{61}$$
$$= 0.688 < 1.0 \quad \textbf{o.k.}$$

CONCLUSIONS

The torsional strength of connection elements can be attributed to the resistance due to uniform torsion, warping torsion, and the Wagner effect. For long members subjected to reasonable torsional rotations, the contribution of both the warping and Wagner torsions are negligible. However, for short members and connection elements, their effect can be significant. If only the elastic uniform (Saint Venant) torsion is considered, the resistance can be significantly underestimated.

For many connection elements, this investigation showed that the torsional strength can be defined as the sum of the plastic uniform torsion strength and the plastic warping strength. For long connection elements, such as extended single-plate connections, the Wagner torsional resistance is negligible at reasonable service rotation limits. However, the Wagner resistance is significant for short connection elements such as conventional single-plate connections, allowing torsional effects to be neglected for these connections.

A method has been proposed for the ultimate strength design of rectangular connection elements subjected to any possible combination of loads, including torsion. The design method results in a significant increase in torsional strength compared to traditional analysis methods. Several design examples showed the proper application of the proposed design method.

For nonstiffened extended single-plate connections, the design procedure in the AISC *Manual* (AISC, 2017) implicitly limits excessive torsional rotations. For connections subjected only to shear loads, the proposed design method results in strengths similar to the AISC *Manual* procedure by explicitly considering torsional effects. The proposed method can also be used to analyze extended single-plate connections subjected to axial forces and out-of-plane forces.

SYMBOLS

B	Amplification factor for second-order torsional effects
C_b	Lateral-torsional buckling modification factor
C_w	Warping constant, in.^{6}
E	Modulus of elasticity, ksi
F	Horizontal couple force, kips
F_{cr}	Critical stress, ksi
F_y	Specified minimum yield strength, ksi
F_{wy}	Horizontal couple force required to initiate first yield, kips
G	Shear modulus of elasticity = 11,200 ksi
I_e	Moment of inertia for the equivalent beam, in.^{4}
I_n	Wagner constant, in.^{6}
J	Torsional constant, in.^{4}
L	Member length, in.
M_{cr}	Elastic critical buckling moment for strong-axis flexure, kip-in.
M_{cx}	Available flexural strength about the x-axis, kip-in.
M_{cy}	Available flexural strength about the y-axis, kip-in.
M_{nx}	Strong-axis flexural strength, kip-in.
M_p	Plastic flexural strength, kip-in.
M_{pe}	Plastic flexural strength of the equivalent beam, kip-in.
M_{px}	Plastic flexural strength about the x-axis, kip-in.

M_{py} Plastic flexural strength about the y-axis, kip-in.

M_{re} Required moment for the equivalent beam, kip-in.

M_{rx} Required x-axis flexural strength, kip-in.

M_{ry} Required y-axis flexural strength, kip-in.

M_{ye} Yield moment of the equivalent beam, kip-in.

P_c Available axial strength, kips

P_r Required axial strength, kips

P_y Axial yield load, kips

R_r Required beam end shear reaction, kips

R_c Calculated shear strength, kips

R_e Approximate experimental shear load where the load-deflection curve became nonlinear, kips

R_u Maximum experimental shear load, kips

S_x Elastic section modulus about the x-axis, in.^{3}

T_1 First-order torsional moment, kip-in.

T_2 Second-order torsional moment, kip-in.

T_b Torsional resistance provided by a top flange lateral brace, kip-in.

T_c Available torsional strength, kips

T_e Sum of the Wagner torsional moment and the uniform torsional moment, kip-in.

T_n Wagner torsional moment, kip-in.

T_p Plastic torsional moment, kip-in.

T_r Required torsional moment, kip-in.

T_u Uniform torsional moment, kip-in.

T_{up} Plastic uniform torsional moment, kip-in.

T_{uy} First-yield uniform torsional moment, kip-in.

T_w Warping torsional moment, kip-in.

T_{wi} Inelastic warping torsional moment, kip-in.

T_{wp} Plastic warping torsional moment, kip-in.

T_{wy} First-yield warping torsional moment, kip-in.

V_c Available shear strength, kips

V_p Plastic shear strength, kips

V_r Required shear strength, kips

W_{nc} Normalized warping function at the corner of the cross section, in.^{2}

a Constant as defined by Equation 15, in.

c Distance to outermost fiber, in.

d Member depth, in.

e Horizontal eccentricity for a single-plate connection, in.

h Distance between couple forces, F, in.

k Exponent applied to the axial load ratio

t Member thickness, plate thickness, in.

t_w Beam web thickness, in.

z Distance along the member length, in.

αd Effective depth of the equivalent cross section, in.

β Normalized increase in torsional resistance due to the Wagner effect

δ Deflection of equivalent beam

δ_y Yield deflection of equivalent beam

τ_y Shear yield stress = $0.6F_y$, ksi

θ Angle of rotation, rad

θ_i Inelastic angle of rotation, rad

θ_u Angle of rotation for uniform torsion, rad

θ_{uy} First-yield angle of rotation for uniform torsion, rad

θ_w Angle of rotation for warping, rad

θ_{wy} First-yield angle of rotation for warping, rad

θ_1 First-order torsional rotation, rad

θ_2 Second-order torsional rotation, rad

θ' Angle of rotation per unit length, first derivative of θ with respect to z, rad/in.

θ'' Second derivative of θ with respect to z, rad/in.^{2}

θ''' Third derivative of θ with respect to z, rad/in.^{3}

σ_n Axial stress developed by the Wagner effect, ksi

σ_{nt} Maximum axial stress developed by the Wagner effect, ksi

σ_{wc} Maximum warping normal stress, ksi

REFERENCES

Abou-Zidan, A. (2014), *Finite Element Study on Unstiffened Extended Single Plate Shear Connections*, Master's Thesis, Dalhousie University, Halifax, Nova Scotia.

AISC (2016), *Specification for Structural Steel Buildings*, ANSI/AISC 360–16, American Institute of Steel Construction, Chicago, IL.

AISC (2017), *Steel Construction Manual*, 15th Ed., American Institute of Steel Construction, Chicago, IL.

Ashkinadze, K. (2008), "Proposals for Limit States Torsional Strength Design of Wide-Flange Steel Members," *Canadian Journal of Civil Engineering*, Vol. 35, pp. 200–209.

Baba, S. and Kajita, T. (1982), "Plastic Analysis of Torsion of a Prismatic Beam," *International Journal for Numerical Methods in Engineering*, Vol. 18, pp. 927–944.

Balaz, I. and Kolekova, Y. (2002), "Warping," *Stability and Ductility of Steel Structures*, Proceedings of the Otto Halasz Memorial Session, Editor: Ivanyi, M., Akademiai Kiado, Budapest.

Bathe, K.J. and Chaudhary, A. (1982), "On the Displacement Formulation of Torsion of Shafts with Rectangular Cross-Sections," *International Journal for Numerical Methods in Engineering*, Vol. 18, pp. 1565–1580.

Bennetts, I.D., Thomas, I.R. and Grundy, P. (1981), "Torsional Stiffness of Shear Connections," *Proceedings of the Metal Structures Congress,* National Committee on Metal Structures of the Institution of Engineers, Australia, Newcastle, May 11–14, pp. 102–106.

Boissonnade, N., Muzeau, J.P. and Villette, M. (2002), "Amplification Effects for Lateral Torsional Buckling," *Stability and Ductility of Steel Structures*, pp. 73–80.

Cook, R.D. and Young, W.C. (1985), *Advanced Mechanics of Materials*, Macmillan Publishing Company, London, England.

Dinno, K.S. and Merchant, W. (July 1965), "A Procedure for Calculation the Plastic Collapse of I-Sections Under Bending and Torsion," *The Structural Engineer*, Vol. 43, No. 7, pp. 219–221.

Dowswell, B. (2004), "Lateral-Torsional Buckling of Wide Flange Cantilever Beams," *Engineering Journal*, AISC, Vol. 41, No. 2, pp. 85–91.

Dowswell, B. (2015), "Plastic Strength of Connection Elements," *Engineering Journal*, AISC, Vol 52, No. 1, pp. 47–65.

Dowswell, B. (2016), "Stability of Rectangular Connection Elements," *Engineering Journal*, AISC, Vol. 53, No. 4, pp. 171–202.

Gjelsvik, A. (1981), *The Theory of Thin Walled Bars*, John Wiley and Sons.

Goodrich, W. (2005), *Behavior of Extended Shear Tabs in Stiffened Beam-to-Column Web Connections*, Master's Thesis, Vanderbilt University.

Gregory, M. (1960), "The Bending and Shortening Effect of Pure Torque," *Australian Journal of Applied Science*, Vol. 11, pp. 209–216.

Hijaj, M.A. and Mahamid, M. (2017), "Behavior of Skewed Extended Shear Tab Connections Part I: Connection to Supporting Web," *Journal of Constructional Steel Research*, Vol. 128, pp. 305–320.

Kjar, A.R. (1967), "The Axis of Distortion," *International Journal of Mechanical Science*, Vol. 9, pp. 873–883.

Lindner, J. and Glitsch, T. (2005), "Simplified Design of Crane Girders with Open Cross Sections Subjected to Biaxial Bending and Torsion," *Advances in Steel Structures*, Vol. 1, pp. 95–104.

Mahamid, M., Rahman, A. and Ghorbanpoor, A. (2007), "The Analysis of Extended Shear Tab Connections Part II: Stiffened Connections," *Engineering Journal*, AISC, Vol. 44, No. 2, pp. 133–145.

May, I.M. and Al-Shaarbaf, I.A.S. (1989), "Elasto-Plastic Analysis of Torsion Using a Three-Dimensional Finite Element Model," *Computers and Structures*, Vol. 33, No. 3, pp. 667–678.

Moore, W.E. and Mueller, K.M. (2002), "Technical Note: Torsional Analysis of Steel Sections," *Engineering Journal*, AISC, Vol. 39, No. 4, pp. 182–188.

Moore, D.B., and Owens, G.W. (February 1992), "Verification of Design Methods for Finplate Connections," *The Structural Engineer,* Vol. 70, No. 3/4.

Muir, L.S. and Hewitt, C.M. (2009), "Design of Unstiffened Extended Single-Plate Shear Connections," *Engineering Journal*, AISC, Vol. 46, No. 2, pp. 67–79.

Neal, B.G. (January 1950), "The Lateral Instability of Yielded Mild Steel Beams of Rectangular Cross-Section," *Philosophical Transactions of the Royal Society of London*, Vol. 242, No. 846, pp. 197–242.

Pastor, T.P. (1977), *Behavior of Beams Loaded both Flexurally and Torsionally*, Master's Thesis, The University of Connecticut, Mansfield, CT.

Pi, Y.L. and Trahair, N.S. (December 1994), "Inelastic Bending and Torsion of Steel I-Beams," *Journal of Structural Engineering*, ASCE, Vol. 120, No. 12, pp. 3397–3417.

Pi, Y.L. and Trahair, N.S. (October 1995), "Plastic-Collapse Analysis of Torsion," *Journal of Structural Engineering*, ASCE, Vol. 121, No. 10, pp. 1389–1395.

Rahman, A., Mahamid, M., Amro, A. and Ghorbanpoor, A. (2007), "The Analysis of Extended Shear Tab Connections Part I: The Unstiffened Connections," *Engineering Journal*, AISC, Vol. 44, No. 2, pp. 117–132.

Reissner, E. and Stein, M. (1951), *Torsion and Transverse Bending of Cantilever Plates*, NACA Technical Note 2369, National Advisory Committee for Aeronautics, June.

Seaburg, P.A. and Carter, C.J. (1997), *Torsional Analysis of Structural Steel Members*, Design Guide 9, AISC, Chicago, IL.

Sherman, D.R. and Ghorbanpoor, A. (2002), *Design of Extended Shear Tabs,* Final Report, American Institute of Steel Construction, Chicago, IL.

Suleiman, M.F. (2013), *Non-Linear Finite Element Analysis of Extended Shear Tab Connections*, Ph.D. Dissertation, University of Cincinnati, Cincinnati, OH.

Timoshenko, S. (1956), *Strength of Materials*, D. Van Nostrand Company.

Thornton, W.A. and Fortney, P.J. (2011), "On the Need for Stiffeners for and the Effect of Lap Eccentricity on Extended Single-Plate Connections," *Engineering Journal*, AISC, Vol. 48, No. 2, pp. 117–125.

Trahair, N.S. (2003), *Non-Linear Elastic Non-Uniform Torsion*, Research Report No. R828, Center for Advanced Structural Engineering, University of Sydney, Sydney, Australia, June.

Trahair, N.S., Bradford, M.A., Nethercot, D.A. and Gardner, L. (2008), *The Behavior and Design of Steel Structures to EC3*, 4th Ed., Taylor and Francis.

Trahair, N.S. and Teh, L.H. (2000), *Second Order Moments in Torsion Members*, Research Report No. R800, Centre for Advanced Structural Engineering, University of Sydney, Sydney, Australia.

Wagner, H. (1936), *Torsion and Buckling of Open Sections*, NACA Technical Memorandum No. 807, National Advisory Committee for Aeronautics.

Wittrick, W.H. (1952), "Lateral Instability of Rectangular Beams of Strain-Hardening Material Under Uniform Bending," *Journal of the Aeronautical Sciences*, Vol. 19, No. 12, December, pp. 835–843.

Zahn, J.J. (1984), "Loss of Torsional Stiffness Caused by Beam Loading," *Journal of Structural Engineering*, ASCE, Vol. 110, No. 1, January, pp. 47–54.